# Pilot design for channel estimation in Doubly Selective Channel

Kushal Anand*, Yong Liang Guan*, Zilong Liu**, Yang Yang† , Zhengchun Zhou†, Pingzhi Fan†, Erry Gunawan*

*School of Electrical and Electronic Engineering, Nanyang Technological University, Singapore
**Institute for Communication Systems, Univ. of Surrey, UK
†Southwest Jiaotong University, Chengdu, China
Email: kanand@ntu.edu.sg

***Abstract*—We consider pilot sequence designs for channel estimation in doubly-selective channels (DSC) which are modeled using the basis expansion model (BEM) approach. We propose to use pilot *sequences* (instead of impulse pilots) to reduce the peak-to-average power ratio (PAPR) of the transmitted signal. Specifically, by analysing the mean square error (MSE) metric of the BEM channel coefficients, we propose the use of Huffman sequences to reduce the PAPR during channel estimation. Furthermore, we show that a systematic re-arrangement of the pilot sequence within the transmission frame can significantly improve the channel estimation performance of the system, as compared to the conventional periodic pilot placement.**

## I. Introduction

In wireless communications, often we need to deal with time-varying channels in which the notorious Doppler shifts/spreads (frequency dispersiveness) are caused by moving transmitters, receivers, or signal reflectors [1]. Furthermore, multipath propagation leads to high frequency selectivity (time dispersiveness) [2]. Such channels with high Doppler and large multipaths are referred to as doubly selective channels (DSC). Due to the large dispersion in the time and frequency domain, channel estimation for the DSC becomes a very challenging task.

Various methods for channel modeling and estimation of DSC have been proposed in the literature [2]–[7]. A common approach adopted in these papers is the modeling of DSC using the BEM in which the time varying channel of each multipath is expressed as a weighted combination of appropriate basis functions such as exponential [2], [3], prolate [8], polynomial [9] etc. Since these basis functions are already known, the receiver just needs to estimate the weights of the bases or the so-called BEM coefficients. Since BEM coefficients are much lesser in number, the channel estimation problem is greatly simplified as we no longer need to estimate each channel coefficient.

We consider single-carrier (time-domain) data transmission and adopt the exponential basis functions for modeling the single-carrier DSC. In most of the current works on single- and multi-carrier transmissions, pilots need to be inserted in the transmission block periodically to sample the time varying channel so that the BEM coefficients can be estimated appropriately. However, in all these works, *impulse* based pilots are used for channel estimation (CE) as shown in Fig. 1. A major drawback of the impulse pilot is that its high peak-to-average power ratio (PAPR) may result in degradation of the transmission power efficiency, hence reducing the transmission range [10].

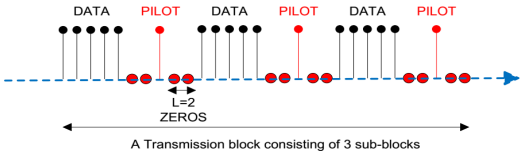


Fig. 1: A transmission block consisting of three sub-blocks, each containing a time-domain Kronecker delta (TDKD) pilot cluster. Each impulse pilot is surrounded by $L$ zeros on both sides, where $L$ denotes the number of multi paths.

In this work, we consider *sequence*-based pilots for CE in DSC. This allows us to spread the power of the impulse pilots in conventional schemes over a number of pilot samples, thereby reducing the PAPR of the pilot. Specifically, we propose the use of Huffman sequences as substitutes for impulse pilots for CE. Moreover, based on our analysis, we propose a suitable arrangement of pilot sequences in the transmission frame so that the MSE of CE is further improved.

The rest of the organization of the paper is as follows. In Section II, we provide the system model of data transmission and channel estimation for DSC. In Section III, we provide details of the proposed sequence based pilots for channel estimation and the pilot placement strategy. Simulation results are provided in Section IV and conclusion is given in Section V.

## II. System and Channel Model

### A. System Model

We consider transmission over a DSC with one transmit antenna each at the transmitter and the receiver. A data sequence $x[n]$ of length $N$ is transmitted at a rate of $\frac{1}{T}$ symbols/s over the DSC. The discrete-time baseband equivalent of the received symbol at the $n^{th}$ time instant can be written as:

$$y[n] = \sum_{l=0}^{L} h[n;l]x[n-l] + v[n], \tag{1}$$

where $h[n;l]$ denotes the discrete-time equivalent baseband representation of the DSC, which subsumes the physical multipath channel together with the transmit and receive pulse

shaping filters, $l$ denotes the $l^{th}$ multi-path, $L$ denotes the number of multi paths and is given as $L = \lfloor \frac{\tau_{max}}{T} \rfloor$ with $\tau_{max}$ being the maximum delay spread of the channel, and $v[n]$ denotes the circularly symmetric complex additive white Gaussian noise (AWGN) with $v[n] \sim \mathcal{CN}(0, \sigma_v^2)$.

We adopt a block transmission design where the pilot symbols are multiplexed with the data by suitably placing them in the block, as shown in Fig. 1. In Fig. 1, the transmission block consists of three sub-blocks, each containing a data sub-block (shown in black) and a pilot sub-block (shown in red).

### B. Channel model

The channel $h[n;l]$ is modeled using the CE-BEM [2] where the $l^{th}$ tap of the channel at the $n^{th}$ time-instant is expressed as a weighted combination of the complex exponentials bases functions[1], and is given as:

$$h[n;l] = \sum_{q=0}^{Q} h_q(l) e^{j\omega_q n} + e[n], \tag{2}$$

where $\omega_q$ denotes the $q^{th}$ BEM modeling frequency, $h_q(l)$ $(q \in \{0,1,...,Q\})$ denotes the $q^{th}$ weight or the $q^{th}$ BEM coefficient corresponding to the $l^{th}$ $(l = 1,...,L)$ path, and $Q := 2\lceil f_{max} N T \rceil$ denotes the number of BEM coefficients, $f_{max}$ being the maximum Doppler spread. Finally, $e[n]$ denotes the modeling error for the above CE-BEM. From (2), it seems that a higher $Q$ can result in better approximation of the BEM to the actual channel and the modeling error is reduced. However, for practical wireless channels, simply increasing $Q$ cannot reduce the channel modeling error significantly.

In many existing works, the modeling frequency $\omega_q$ is taken to be uniformly distributed between $\left[\frac{2\pi}{N}(\frac{-Q}{2}), \frac{2\pi}{N}(\frac{Q}{2})\right]$ with equal spacing between them, and are given as $\omega_q = \frac{2\pi}{N}(q - \frac{Q}{2})$, $q \in \{0,1,...,Q\}$ [2], [3]. Again, for practical channels, this results in large modeling errors. Therefore, in this work, we use the BEM modeling frequencies ($\omega_q$) mentioned in [5], where the $\omega_q$'s are uniformly distributed between $[-2\pi f_{max} T, +2\pi f_{max} T]$, and provide a much better channel modeling.

## III. Pilot design and Channel estimation

### A. Pilot design

We assume that the data-pilot multiplexed $k^{th}$ transmitted block consists of $P$ sub-blocks, with the $p^{th}$ sub-block consisting of a data vector sub-block $\mathbf{s}_p$ and a pilot vector sub-block $\mathbf{b}_p$, and is given as $\mathbf{x} \triangleq [\mathbf{s}_1^T(k), \mathbf{b}_1^T(k), ..., \mathbf{s}_P^T(k), \mathbf{b}_P^T(k)]^T$, $\forall k$. Specifically, the pilot cluster in the $p^{th}$ sub-block can be written as:

$$\begin{aligned}\mathbf{b}_p &= [\underbrace{b_{p,0}, ..., b_{p,(L-1)}}_{\text{set to zeros}}, b_{p,L}, ..., b_{p,L+M-1}, \underbrace{b_{p,L+M} ..., b_{p,(N_p-1)}}_{\text{set to zeros}}]^T \\ &= [0,0,...0,, b_{p,L}, ..., b_{p,L+M-1}, 0,0,...0]^T, \end{aligned} \tag{3}$$

[1] Note that different bases can be used to model the channel such as the most popular Fourier bases [6], prolate bases [8], polynomial bases [9], each having its own advantages and drawbacks.

where the first and last $L$ elements of the pilot cluster are set to zeros (as shown above) so as to avoid the inter-symbol interference between the data and the pilot symbols across the sub-block and the main block [2]. In the above, note that $N_p = 2L + M$, where $M$ is the length of the sequence we wish to design. $2L$ comes from the $L$ zeros on either side of the sequence. For "impulse" pilot, $M = 1$ and $N_p = 2L + 1$.

In our proposed approach, unlike [2] and other existing works, the non-zero pilot cluster in the middle of $\mathbf{b}_p$, i.e., $[b_{p,L}, ..., b_{p,L+M-1}]$ is a *sequence* of length $M$, instead of an *impulse*, as shown in Fig. 2. The motivation behind using a sequence as pilot is to reduce the PAPR of the transmitted pilot. We define the PAPR of a time-domain length-$N$ sequence $\mathbf{b}$ with elements $\{b_n\}$ as [11]:

$$PAPR(\mathbf{b}) = \frac{\max\limits_{0 \le n \le N-1} |b_n|^2}{(1/N) \sum\limits_{n=0}^{N-1} |b_n|^2} \tag{4}$$

From (4), the PAPR of the impulse pilot (see Fig. 1), is $2L + 1$. Clearly, by spreading the pilot power over multiple symbols of a sequence, we can reduce the pilot PAPR. However, while using sequences as pilots, one has to ensure that a reduced PAPR of the pilots won't result in performance loss in channel estimation. In this paper, we show next that we can use Huffman sequences as the pilot clusters for reduced PAPR and good channel estimation performance.

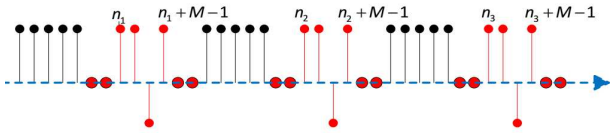


Fig. 2: A transmission block consisting of three sub-blocks, each containing a data sub-block (black) and a sequence-based pilot cluster (red). Each sequence pilot is surrounded by $L = 2$ zeros on both sides, where $L$ denotes the number of multi paths. $n_i$ denotes the "start" position of the length-$M$ sequence in the $i^{th}$ sub-block.

### B. Estimation of BEM coefficients

Using (1) and (2), the received signal can be written in matrix form as:

$$\mathbf{y} = \mathbf{H}\mathbf{x} + \mathbf{v}, \tag{5}$$

where $\mathbf{H} = \sum_{q=0}^{Q} \mathbf{D}_q \mathbf{H}_q$, $\mathbf{D}_q = diag[1, e^{j\omega_q}, ..., e^{j\omega_q (N-1)}]$, and $\mathbf{H}_q$ is a lower triangular Toeplitz matrix with first column $[h_q(0), ..., h_q(L), 0, ..., 0]^T$, and $\mathbf{v}$ consists of the AWGN components, i.e., $v[n]$ defined in Section II-A. Due to the zero-padding on both sides of the pilot sequence, (5) can be clearly segregated into separate data and the pilot equations ($\mathbf{y}_s$ and $\mathbf{y}_b$ respectively) with corresponding channel matrices $\mathbf{H}_s$ and $\mathbf{H}_b$, and noise vectors $\mathbf{v}_s$ and $\mathbf{v}_b$, as shown below:

$$\mathbf{y}_s = \mathbf{H}_s \mathbf{s} + \mathbf{v}_s, \tag{6}$$

$$\mathbf{y}_b = \mathbf{H}_b \mathbf{b} + \mathbf{v}_b, \tag{7}$$

where $\mathbf{s} \triangleq [\mathbf{s}_1^T, ..., \mathbf{s}_P^T]$, and $\mathbf{b} \triangleq [\mathbf{b}_1^T, ..., \mathbf{b}_P^T]^T$.

Focussing on channel estimation, we can write (7) as:

$$\mathbf{y}_b = \sum_{q=0}^{Q} \begin{bmatrix} \mathbf{D}_{q,1}\mathbf{H}_{q,1}\mathbf{b}_1 \\ \vdots \\ \mathbf{D}_{q,P}\mathbf{H}_{q,P}\mathbf{b}_P \end{bmatrix} + \mathbf{v}_b, \tag{8}$$

where $\mathbf{D}_{q,p}$ and $\mathbf{H}_{q,p}$ correspond to the sub matrices from $\mathbf{D}_q$ and $\mathbf{H}_q$ (shown below (5)). Specifically, $\mathbf{D}_{q,p}$ $(q \in \{0,1,...,Q\},\ p \in \{1,2,...,P\})$ for the $q^{th}$ BEM frequency and the $p^{th}$ sub-block can be written as:

$$\mathbf{D}_{q,p} = \begin{bmatrix} e^{j\omega_q(n_p)} & 0 & \cdots & 0 \\ 0 & e^{j\omega_q(n_p+1)} & \cdots & 0 \\ \vdots & \vdots & \ddots & \vdots \\ 0 & 0 & \cdots & e^{j\omega_q(n_p+N_p-L-1)} \end{bmatrix}, \tag{9}$$

where $n_p \in \{1,...,N\}$ denotes the start position of the $p^{th}$ non-zero pilot symbol in the transmission block (see Fig. 2).

Next, define a pilot matrix $\mathbf{B}_p$ as

$$\begin{bmatrix} b_{p,L} & \cdots & b_{p,0} \\ \vdots & \ddots & \vdots \\ b_{p,N_p-1} & \cdots & b_{p,N_p-L-1} \end{bmatrix}, \tag{10}$$

then, it can be verified that $\mathbf{H}_{q,p}\mathbf{b}_p = \mathbf{B}_p\mathbf{h}_q$ [2]. Denoting $\mathbf{h}_q \triangleq [h_q(0),...,h_q(L)]^T$, and $\mathbf{h} \triangleq [\mathbf{h}_0^T,...,\mathbf{h}_Q^T]^T$, we can finally write the pilot equation (8) as:

$$\mathbf{y}_b = \mathbf{\Phi}\mathbf{h} + \mathbf{v}, \tag{11}$$

where $\mathbf{\Phi}$ is defined as:

$$\begin{bmatrix} \mathbf{D}_{0,1}\mathbf{B}_1 & \cdots & \mathbf{D}_{Q,1}\mathbf{B}_1 \\ \vdots & \ddots & \vdots \\ \mathbf{D}_{0,P}\mathbf{B}_P & \cdots & \mathbf{D}_{Q,P}\mathbf{B}_P \end{bmatrix}, \tag{12}$$

From (11), the MSE channel estimation of the BEM coefficient vector $\widehat{\mathbf{h}}$ is given as:

$$\widehat{\mathbf{h}} = (1/\sigma_v^2)(\mathbf{\Gamma}^{-1} + (1/\sigma_v^2)\mathbf{\Phi}^H\mathbf{\Phi})^{-1}\mathbf{\Phi}\mathbf{y}_b, \tag{13}$$

where the BEM correlation matrix $\mathbf{\Gamma} = \mathbb{E}\{\mathbf{h}\mathbf{h}^H\}$ is assumed to be known at the receiver. The channel estimation MSE is then given as:

$$MSE \triangleq tr((\mathbf{\Gamma}^{-1} + (1/\sigma_v^2)\mathbf{\Phi}^H\mathbf{\Phi})^{-1}). \tag{14}$$

Now, in order to minimize the MSE, we need to design the sequences $\mathbf{b}_p$ (or $\mathbf{B}_p$) so that the MSE matrix $\mathbf{\Phi}^H\mathbf{\Phi}$ is diagonal or close to diagonal [12]. At this point, it is important to note that $\mathbf{\Phi}^H\mathbf{\Phi}$ is perfectly diagonal only if periodic placement of pilot is done, the transmission block length $N$ is an integer multiple of the number of sub-blocks, and the BEM frequency $\omega_q$ is uniformly distributed between $\left[\frac{2\pi}{N}(\frac{-Q}{2}), \frac{2\pi}{N}(\frac{Q}{2})\right]$, i.e., $\omega_q = \frac{2\pi}{N}(q - \frac{Q}{2}),\ q \in \{0,1,...,Q\}$. However, for practical channels (such as Jakes'), $\omega_q = \frac{2\pi}{N}(q - \frac{Q}{2})$ can not model the channel accurately (results in large modeling errors), and thus perfectly diagonal MSE matrix is not possible, leading to poor CE.

For more accurate BEM modeling of the channels as in [5], *generally*, the off-diagonal elements of $\mathbf{\Phi}^H\mathbf{\Phi}$ are non-zeros. Therefore, we aim for pilot designs such that the off-diagonal elements are reduced in magnitude, possibly to a very small value. Next, we can expand $\mathbf{\Phi}^H\mathbf{\Phi}$ as:

$$\begin{bmatrix} \sum_{i=1}^{P}\mathbf{B}_i^H\mathbf{D}_{0i}^H\mathbf{D}_{0i}\mathbf{B}_i & \sum_{i=1}^{P}\mathbf{B}_i^H\mathbf{D}_{0i}^H\mathbf{D}_{1i}\mathbf{B}_i & \cdots & \sum_{i=1}^{P}\mathbf{B}_i^H\mathbf{D}_{0i}^H\mathbf{D}_{Qi}\mathbf{B}_i \\ \sum_{i=1}^{P}\mathbf{B}_i^H\mathbf{D}_{1i}^H\mathbf{D}_{0i}\mathbf{B}_i & \sum_{i=1}^{P}\mathbf{B}_i^H\mathbf{D}_{1i}^H\mathbf{D}_{1i}\mathbf{B}_i & \cdots & \sum_{i=1}^{P}\mathbf{B}_i^H\mathbf{D}_{1i}^H\mathbf{D}_{Qi}\mathbf{B}_i \\ \vdots & \vdots & \ddots & \vdots \\ \sum_{i=1}^{P}\mathbf{B}_i^H\mathbf{D}_{Qi}^H\mathbf{D}_{0i}\mathbf{B}_i & \sum_{i=1}^{P}\mathbf{B}_i^H\mathbf{D}_{Qi}^H\mathbf{D}_{1i}\mathbf{B}_i & \cdots & \sum_{i=1}^{P}\mathbf{B}_i^H\mathbf{D}_{Qi}^H\mathbf{D}_{Qi}\mathbf{B}_i \end{bmatrix}, \tag{15}$$

From (15), diagonalizing the MSE matrix $\mathbf{\Phi}^H\mathbf{\Phi}$ is equivalent to solving the following two equations:

$$\sum_{i=1}^{P}\mathbf{B}_i^H\mathbf{D}_{0i}^H\mathbf{D}_{0i}\mathbf{B}_i = \sum_{i=1}^{P}\mathbf{B}_i^H\mathbf{B}_i = \mathcal{P}\mathbf{I}, \tag{16}$$

$$\sum_{i=1}^{P}\mathbf{B}_i^H\mathbf{D}_{q_1i}^H\mathbf{D}_{q_2i}\mathbf{B}_i = 0,\ q_1 \neq q_2, \tag{17}$$

where $\mathcal{P}$ denotes the power allocated to the pilot sequence in the transmitted block. Clearly, (16) shows that the $P$ pilot sequences $\{\mathbf{b}_1, \mathbf{b}_2, \cdots, \mathbf{b}_P\}$ should form a complementary set of sequences [13] having zero aperiodic autocorrelation sums. Indeed, if we use Golay complementary pairs (GCPs) [14] as pilot sequences every two consecutive sub-blocks[2], (16) is satisfied. However, such GCPs cannot ensure (17) can be always satisfied. At this point, we note that (16) can also be satisfied by sequences with impulse-like autocorrelation functions. Thus, we propose to use Huffman sequence as another potential sequence candidate which satisfies (16). An interesting property of Huffman sequence is that its aperiodic autocorrelation sequence is almost impulse-like with zero sidelobes at all shifts except at the last one [15]. An autocorrelation example of a length-5 Huffman sequence is shown in Fig. 3.

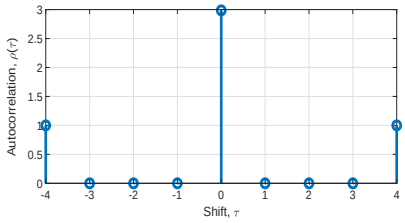


Fig. 3: Autocorrelation function of a Huffman sequence of length-5.

From the Huffman autocorrelation property, we observe that for length-$N$ Huffman sequences, zero autocorrelation sidelobes can be observed for up to $(N-2)$ shifts. Thus, if we have a DSC with $L$ multipaths, we have the main diagonal submatrix $\mathbf{B}_i^H\mathbf{B}_i$ in (16) of size $(L+1)\times(L+1)$ (can be verified)

[2] For example, consider the GCPs $\mathbf{g}_1, \mathbf{g}_2$, and a data transmission frame consisting of 4 sub-blocks. Then, the transmission frame can be represented as $[\mathbf{s}_1, \mathbf{g}_1, \mathbf{s}_2, \mathbf{g}_2, \mathbf{s}_3, \mathbf{g}_1, \mathbf{s}_4, \mathbf{g}_2]^T$, where $[\mathbf{s}_i, \mathbf{g}_j]^T$ denotes a sub-block comprising a data vector $\mathbf{s}_i$ and a pilot sequence vector $\mathbf{g}_j$. Also, note that in this case, $P$ should be even.

which should be a scaled identity matrix (see (16)) with $L$ zero elements in every row. Therefore, we need Huffman sequences of length at least $(L+2)$. For example, for number of multi paths, $L=3$, we need a length-5 Huffman sequence pilot cluster, denoted as $[b_1, b_2, b_3, b_4, b_5]^T$, and the overall pilot cluster is given as $\mathbf{b} = [0,0,0,b_1,b_2,b_3,b_4,b_5,0,0,0]^T$.

The explicit generation of Huffman sequences has not been mentioned in this paper, and interested readers are referred to [15]. It is worth noting that we may have several Huffman sequences that satisfy (16). Since our objective is to reduce the PAPR of the pilots, therefore, we choose the Huffman sequence with low PAPR. From [15], it can be seen that searching for the Huffman sequence with low PAPR is not computationally expensive. The details are omitted from this paper. It is worth noting that we use the same Huffman sequence based pilot cluster in all the sub-blocks, i.e., $[\mathbf{0}_{1\times L}, b_L, ..., b_{L+M-1}, \mathbf{0}_{1\times L}]^T,\ \forall p$ (see (3)).

Once Huffman sequences are applied as the pilots, one has to ensure that the off-diagonal sub matrices' elements in (15) are reduced in magnitude (zero matrices in the best case). An interesting observation is that we can design the sequences or sequence matrices $\mathbf{B}_i$ to satisfy (16) whereas we can design the matrices $\mathbf{D}_{qi}$ separately to satisfy (17). Thus, choosing Huffman sequences to satisfy (16) does not affect the design criteria in (17) which we discuss next.

Note that the sub-matrix $\mathbf{F}_{q_1,q_2} \triangleq \sum_{i=1}^{P} \mathbf{B}_i^H \mathbf{D}_{q_1 i}^H \mathbf{D}_{q_2 i} \mathbf{B}_i$ $(q_1 \neq q_2)$ in (15) is a $(L+1)\times(L+1)$ matrix, and it can be verified that there are $Q$ such sub matrices in the first row of (15) which determine all the equations of (17). Thus, we need to analyse only the $Q$ sub matrices in the first row of (15). On analysing *each element* of the sub-matrix $\mathbf{F}_{q_1,q_2},\ (q_1 \neq q_2),\ q_1, q_2 \in \{0,...,Q\}$, we get the following equations:

$$\rho_{q_1 q_2}(\tau) = \sum_{p=1}^{P} \sum_{i=L}^{L+M-1} b_{i+\tau}^{\star} b_i e^{j\Delta_{q_1 q_2}(n_p+i+\tau-L)},\ \tau = 0,..,L, \tag{18}$$

where $\rho_{q_1 q_2}(\tau) = [\mathbf{F}_{q_1,q_2}]_{1,\tau}$, i.e., the $\tau^{th}$ $(\tau \neq 0)$ element of the first row of $\mathbf{F}_{q_1,q_2}$, and $\Delta_{q_1 q_2} = (\omega_{q_2} - \omega_{q_1})$. Now, for $\tau = 0$, (18) can be expanded as: $\rho_{q_1 q_2}(0) =$

$$b_L^{\star} b_L \sum_{p=1}^{P} e^{j\Delta_{q_1 q_2} n_p} + b_{L+1}^{\star} b_{L+1} e^{j\Delta_{q_1 q_2}} \sum_{p=1}^{P} e^{j\Delta_{q_1 q_2} n_p} + \cdots$$
$$+ b_{L+M-1}^{\star} b_{L+M-1} e^{j(M-1)\Delta_{q_1 q_2}} \sum_{p=1}^{P} e^{j\Delta_{q_1 q_2} n_p}. \tag{19}$$

It can be verified that if $(\sum_{p=1}^{P} e^{j\Delta_{q_1 q_2} n_p})$ in $\rho_{q_1 q_2}(0)$ in (19) becomes zero, $\rho_{q_1 q_2}(\tau),\ \tau \neq 0$ also become zeros. However, we need to make the $\rho_{q_1 q_2}(0)$ to zero for all $q_1, q_2$, i.e., for all the sub matrices $\mathbf{F}_{q_1,q_2},\ (q_1 \neq q_2),\ q_1, q_2 \in \{0,...,Q\}$.

From (19), we note that $\rho_{q_1 q_2}(0)$ (equivalently, the off-diagonal sub-matrices) may be reduced by changing the placement of the pilot, $n_p$, without disturbing the identity sub matrices (due to the Huffman sequences in (16)) along the main diagonal in (15). Thus, in order to make the off-diagonal matrix values small, we can form the following optimization problem.

$$\min_{n_p\ \forall p} \left| \sum_{p=1}^{P} e^{j\Delta_{q_1 q_2} n_p} \right|,\ \forall \Delta_{q_1 q_2},\ q_1, q_2 \in \{0,...,Q\}, q_1 \neq q_2. \tag{P1}$$
$$s.t.\ \ |n_p - n_{p'}| \geq (L+M), p \neq p'$$
$$n_P + M \leq (N - L + 1).$$

The first constraint implies that the "starting" non-zero pilot symbols of two different pilot clusters should be separated by at least $(L+M)$ (see Fig. 2 for reference). The second constraint arises from the fact that the "last" non-zero pilot symbol in the last pilot cluster should be followed by $L$ zeros.

We assume that the BEM modeling frequencies are equi-spaced (the analysis is valid otherwise also), i.e, $\Delta := (\omega_{q_2} - \omega_{q_1}) = (\omega_{q_3} - \omega_{q_2})$, and so on. Then the problem (P1) can be written as:

$$\min_{n_p\ \forall p} \left| \sum_{p=1}^{P} e^{j\kappa\Delta n_p} \right|,\ \kappa \in \{1,...,Q\}. \tag{P2}$$
$$s.t.\ \text{Constraints in (P1).}$$

In the above optimization problem, for $\kappa = i$, magnitude minimization is performed for the $i^{th}$ off-diagonal sub-matrix in the first row of (15). By minimization of $|\sum_{p=1}^{P} e^{j\kappa\Delta n_p}|$, we can reduce the off-diagonal elements of $\mathbf{\Phi}^H\mathbf{\Phi}$, and thereby, aim to minimize the MSE of the channel estimation error by diagonalizing the matrix. It can be noted from the objective in (P2) that the pilot positions in the sub-blocks provide *phase rotations* (sum of exponentials), and the sum of the phases should be minimized in order to minimize the channel estimation MSE.

An alternative approach for pilot placement design would be to directly minimize MSE in (14) by changing the pilot positions [5], [16]. However, direct minimization would be computationally expensive [5] due to the costly matrix inversion operation involved for large matrices. The complexity is further increased due to the integer-programming involved in the problem. On the other hand, by minimizing just the magnitude sum of exponential cost functions in (P2), no matrix inversion operation is involved and thus the search complexity is greatly reduced. Moreover, our approach gives insight into the problem on how the channel estimation can be improved using phase rotations obtained by changing the position of the pilot sequences within the transmission block.

It is noted that (14) is a multi-objective optimization problem (since $\kappa = 1,...,Q$) with $Q$ objectives that need to be simultaneously minimized by changing the pilot positions. It is possible that while we optimize the objective for $\kappa = i$, it may increase for $\kappa = j,\ j \neq i$. Thus, the desired MSE objective in (14) may not be actually minimized. However,

we can obtain a low-complexity sub-optimal MSE minimizing solution by making use of the problem in (P2). To obtain a low-complexity sub-optimal solution, we can evaluate (P2) for each $\kappa = 1, ..., Q$, and then compare the optimized MSE metric (obtained using (14) for each of the $Q$ pilot placement solutions obtained by solving (P2)) with the MSE obtained by the traditional *periodic* pilot placement, and then choose the pilot placement with the minimum MSE.

Note that although the above approach does not give the optimal solution, it provides a very low-complexity approach to channel MSE minimization which performs better than the periodic pilot placement proposed in existing works. Thus, by using an appropriate pilot sequence and low complexity pilot placement design, we can improve the channel MSE significantly, as shown next in the numerical results.

## IV. Simulation Results

In this section, we discuss the simulation results for the proposed low PAPR sequence based pilot design for channel estimation for DSC. The DSC is of order $L = 3$, i.e., four multi paths are considered and the normalized Doppler spread $f_{max}T$ for the fast fading channel is $0.005$. Each channel tap is modeled as an i.i.d. random variable correlated in time according to Jakes' model with the correlation function given as $J_0(2\pi n f_{max} T)$, where $J_0$ is the zeroth-order Bessel function of the first kind. The transmission block length is set to be $N = 99$ symbols for the proposed Huffman sequence-based pilots (also referred to as "sequence pilots"), and thus number of BEM coefficients, $Q = 2\lceil f_{max} N T \rceil = 2$. We also compare the channel estimation results with the case when impulse pilot ("TDKD" pilot structure) is used for channel estimation (see Fig. 1) [2]. The number of sub-blocks (for both sequence and impulse pilots scenario) is chosen to be three.

The average channel gain for each multi path is assumed to be $\frac{1}{L+1}$ so that the overall channel gain is unity. Similar to [2], the signal to noise ratio (SNR) is defined as the average SNR (averaged over all the data and the pilot sub-blocks in the transmission frame), and is given as $\frac{\mathcal{P}_T}{(N-2LP)\sigma_v^2}$, where $\mathcal{P}_T$ is the total power over the entire transmission block and $\sigma_v^2$ is the noise variance, and $P$ is the number of sub-blocks within the transmission frame. We make sure that the number of pilots is sufficient so that the number of equations is more than the number of $(Q+1)(L+1)$ unknown BEM coefficients. The transmission efficiency $\eta$ is assumed to be $2/3$, i.e., the data symbols constitute $66.67\%$ of the transmission frame. For the transmission scenario of sequence-based pilots, we assume that $35\%$ of the total transmission power is allocated to the pilots whereas the rest is given to the data. For fairness of comparison, same pilot power is considered for the impulse pilot based transmission also.

Fig. 4 shows the channel estimation MSE plot obtained using the proposed pilot designs. For the sequence pilot's case, we have used a Huffman sequence of length-5 for the pilot cluster in each sub-block, with $L$ zero padding on either side of the sequence. Thus, the overall pilot cluster length in each sub-block is 11. To maintain $\eta = 2/3$, 22 data symbols are placed in each sub-block (Note that $N = 99$ as mentioned before). For the impulse pilot's case, 3 sub-blocks are considered, with each sub-block consisting of $14$ data symbols and $7$ (one impulse pilot surrounded by $L$ zeros on either side) pilot symbols, totaling to a block length[3] $N = 63$.

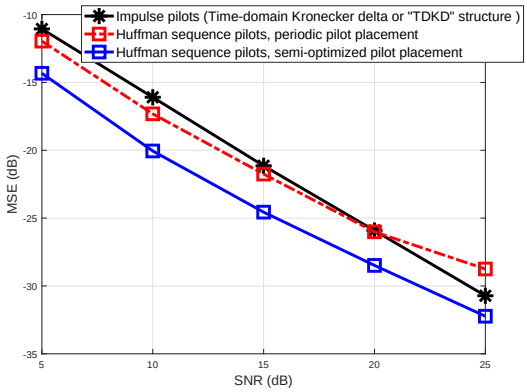


Fig. 4: MSE performances of the Huffman sequence based pilot design with and without pilot placement optimization.

From Fig. 4, note that for the same pilot power, the Huffman sequence pilots provide better channel estimation in the low-to-mid SNR regions, as compared to the impulse pilot's case, but with a lower PAPR of $3.68$ as opposed to 7 for the impulse pilot. Furthermore, our proposed pilot placement strategy "semi-optimized pilot placement" (with the Huffman sequence pilots) provides significantly better channel estimation compared to both the impulse as well as the sequence pilots with traditional periodic pilot placement. For the pilot placement optimization in our current simulations, we have used a low-complexity approach by optimizing the position of the pilot in the first cluster (sub-block) only and for $\Delta_{q_1 q_2} = 1$ in (P2), i.e., for the nearest off-diagonal sub-matrix, and yet significant performance improvement can be observed.

## V. Conclusion

In this paper, we have studied sequence designs to reduce the PAPR of the pilots used for channel estimation of doubly selective fading channels. Using channel estimation error analysis, we have suggested the use of optimized Huffman sequences as the desired pilots for channel estimation. Furthermore, based on our analysis, we have proposed a very low-complexity pilot placement strategy to improve the channel estimation performance, as compared to conventional periodic pilot placement.


## Acknowledgements

This work was supported by the NRF-NSFC project under Grant NRF2016NRF-NSFC001-089. The work of Z. Liu was also supported in part by National Natural Science Foundation of China under Grant 61750110527, a Research Fund for International Young Scientists.


[3] Note that for impulse pilot's case, we need block length $N = 63$ symbols to maintain $\eta = 2/3$.

## REFERENCES


[1] J. Wu and P. Fan, "A survey on high mobility wireless communications: Challenges, opportunities and solutions," *IEEE Access*, vol. 4, pp. 450–476, Jan 2016.

[2] X. Ma, G. B. Giannakis, and S. Ohno, "Optimal training for block transmissions over doubly selective wireless fading channels," *IEEE Trans. Signal Process.*, vol. 51, no. 5, pp. 1351–1366, May 2003.

[3] G. Leus, "On the estimation of rapidly time-varying channels," in *Proc. IEEE European signal Processing Conference (EUSIPCO)*, Sept 2004, pp. 2227–2230.

[4] F. Qu and L. Yang, "On the estimation of doubly-selective fading channels," *IEEE Trans. Wireless Commun.*, vol. 9, no. 4, pp. 1261–1265, April 2010.

[5] T. Whitworth, M. Ghogho, and D. McLernon, "Optimized training and basis expansion model parameters for doubly-selective channel estimation," *IEEE Trans. Wireless Commun.*, vol. 8, no. 3, pp. 1490–1498, March 2009.

[6] J. K. Tugnait, S. He, and H. Kim, "Doubly selective channel estimation using exponential basis models and subblock tracking," *IEEE Trans. Signal Process.*, vol. 58, no. 3, pp. 1275–1289, March 2010.

[7] Z. Sheng, H. D. Tuan, H. H. Nguyen, and Y. Fang, "Pilot optimization for estimation of high-mobility ofdm channels," *IEEE Trans. Veh. Technol.*, vol. 66, no. 10, pp. 8795–8806, Oct 2017.

[8] T. Zemen and C. F. Mecklenbrauker, "Time-variant channel estimation using discrete prolate spheroidal sequences," *IEEE Trans. Signal Process.*, vol. 53, no. 9, pp. 3597–3607, Sept 2005.

[9] H. Hijazi and L. Ros, "Polynomial estimation of time-varying multipath gains with intercarrier interference mitigation in ofdm systems," *IEEE Trans. Veh. Technol.*, vol. 58, no. 1, pp. 140–151, Jan 2009.

[10] A. Goldsmith, *Wireless Communications*. Cambridge University Press, 2005.

[11] S. Hu, Z. Liu, Y. L. Guan, W. Xiong, G. Bi, and S. Li, "Sequence design for cognitive cdma communications under arbitrary spectrum hole constraint," *IEEE J. Sel. Areas Commun.*, vol. 32, no. 11, pp. 1974–1986, November 2014.

[12] S. Ohno and G. B. Giannakis, "Capacity maximizing mmse-optimal pilots for wireless ofdm over frequency-selective block rayleigh-fading channels," *IEEE Trans. Inf. Theory*, vol. 50, no. 9, pp. 2138–2145, Sept 2004.

[13] C.-C. Tseng and C. Liu, "Complementary sets of sequences," *IEEE Trans. Inf. Theory*, vol. 18, no. 5, pp. 644–652, Sep. 1972.

[14] M. Golay, "Complementary series," *IRE Trans. Inf. Theory*, vol. 7, no. 2, pp. 82–87, Apr. 1961.

[15] P. Fan and M. Darnell, *Sequence design for communications applications*. Research Studies Press, 1996.

[16] J. Oh, J. Kim, and J. Lim, "On the design of pilot symbols for ofdm systems over doubly-selective channels," *IEEE Commun. Lett.*, vol. 15, no. 12, pp. 1335–1337, Dec. 2011.